

## He–Xe microdischarges: Comparison of simulation results with experimental data

G. Veronis, U. S. Inan,<sup>a)</sup> and V. P. Pasko<sup>b)</sup>

Space, Telecommunications, and Radioscience Laboratory, Stanford University, Stanford, California 94305

(Received 7 August 2000; accepted for publication 8 November 2000)

A comparison of predictions of a one-dimensional simulation model with the results of a recent experimental study [Appl. Phys. Lett. **76**, 544 (2000)] of a dc He–Xe microdischarge is presented. The experimental results are remarkably reproduced by the model but only when unusually high values are used for the unknown rate coefficients of formation and recombination reactions of  $\text{HeXe}^+$  heteronuclear ions. © 2001 American Institute of Physics. [DOI: 10.1063/1.1338494]

Plasma display panels (PDPs) are one of the leading candidates in the competition for large-size, high-brightness flat-panel displays, suitable for high-definition television (HDTV) monitors.<sup>1,2</sup>

Gas mixtures of He/Xe or Ne/Xe are typically used in PDPs. One of the major challenges in research related to PDPs is the optimization of the gas mixture composition and pressure. The present level of understanding of the complicated kinetic processes which determine the efficiency and the emission output of the discharge is still not satisfactory in the case of inert gas mixtures.<sup>3</sup> Computer simulations are effective in identifying the basic properties of the discharge and the dominant mechanism of VUV emission. Experimental studies of plasma discharges in PDPs are extremely difficult due to the very small cell dimensions and complicated panel structure. However, measurements in simpler geometries with similar dimensions and gas mixture compositions as in actual PDPs, can contribute to the understanding of the kinetics of inert gas mixtures. Such measurements can also be used for the validation of simulation models. In this letter, we present a comparison of predictions of a one-dimensional simulation model with the results of a recent experimental study of a He–Xe microdischarge.<sup>4</sup>

The model utilized here is one-dimensional and is based on self-consistent simulation of a dc microdischarge, similar to those previously developed by Meunier, Belenguer, and Boeuf<sup>5</sup> and Punset, Boeuf, and Pitchford,<sup>6</sup> with the difference that the external circuit consists of a resistor rather than capacitive dielectric layers, as in their cases. The space and time variation of the electric field within the gap is self-consistently determined by solving the fluid equations for ions ( $\text{He}^+$ ,  $\text{Xe}^+$ ,  $\text{He}_2^+$ ,  $\text{Xe}_2^+$ ,  $\text{HeXe}^+$ ) and electrons together with Poisson's equation, subject to the boundary conditions imposed by the electrode boundaries. The steady-state solution is determined iteratively using a technique similar to that described by Boeuf.<sup>7</sup> For numerical stability purposes, the current in the circuit is set to be equal to the conduction current at a plane between the electrodes.<sup>7</sup> The transient evolution of the calculated current and voltage across the gap is, therefore, not correct during iterations, but the calculated

steady-state values are exact. The electrical model is coupled to a model of excited species kinetics and UV emission. The electron-impact ionization and excitation frequencies as well as the electron drift velocity are calculated as a function of the reduced electric field  $E/N$  using the Boltzmann code ELENDF.<sup>8</sup> Electron–atom collision cross sections for He and Xe are taken from the SIGLO Series.<sup>9</sup> Ion mobilities and rate coefficients for Penning ionization, dimer ions formation, charge exchange, recombination, and neutral kinetics reactions, as well as excited species lifetimes, are taken from the literature.<sup>3,5,10–15</sup> As in Meunier, Belenguer, and Boeuf,<sup>5</sup> a Holstein escape factor is used to describe the lengthening of the apparent lifetime of the resonant state  $\text{Xe}^*(^3P_1)$  due to radiation trapping, and the resonance radiation is assumed to be optically thin.<sup>16</sup> In Fig. 1, we show the ionization efficiency  $\eta$  ( $=\alpha/E$ , where  $\alpha$  is the first Townsend coefficient) as a function of  $E/p$  for pure He, 10% Xe in He, and pure Xe, calculated using ELENDF. Our calculations are in good agreement with Uchida *et al.*,<sup>17</sup> and the experimental values of Takahashi and Tachibana.<sup>18</sup>

The measured current–voltage characteristics for various He–Xe mixtures at 250 Torr and an electrode spacing of 250  $\mu\text{m}$  are reported by Postel and Cappelli.<sup>4</sup> In order to compare our simulation results with these measurements, we chose the electrode surface used in the determination of the current, and the value of the external resistor to be the same as in the

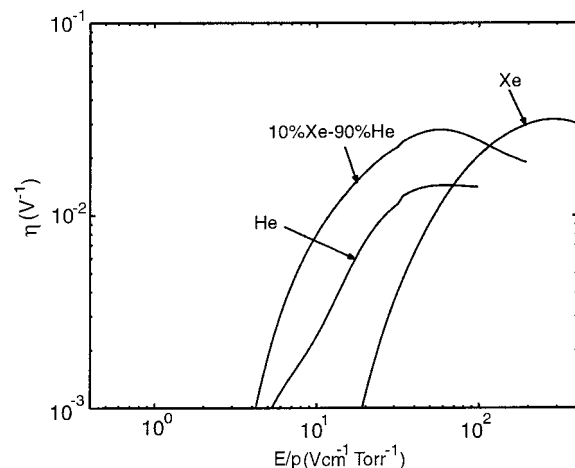


FIG. 1. Ionization efficiency  $\eta$  for different mixture compositions.

<sup>a)</sup>Electronic mail: inan@nova.stanford.edu

<sup>b)</sup>Present address: Communications and Space Sciences Laboratory, The Pennsylvania State University, University Park, PA 16802.

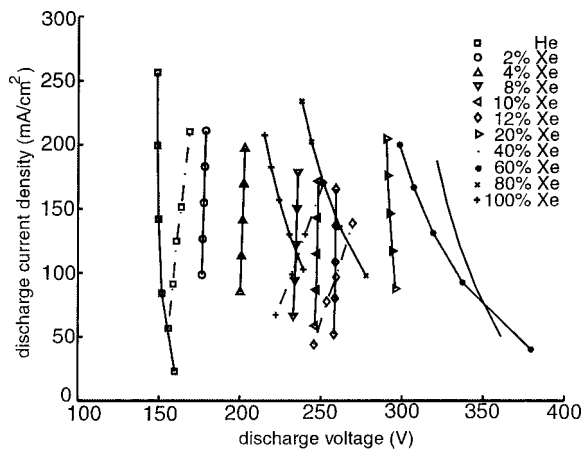


FIG. 2. Calculated  $V$ - $I$  characteristics for various He-Xe mixtures at 250 Torr and electrode spacing of 250  $\mu\text{m}$ . Some experimental  $V$ - $I$  characteristics are shown with a dashed line for comparison.

experimental setup.<sup>4</sup> In addition, the secondary electron emission coefficients for  $\text{He}^+$ ,  $\text{He}_2^+$  and  $\text{Xe}^+$ ,  $\text{Xe}_2^+$  ions were determined by the measured breakdown voltages for pure He and pure Xe for  $pd=6.25$  cm Torr, corresponding to the  $V$ - $I$  characteristics measurements, yielding  $\gamma_{\text{He}}=2\gamma_{\text{He}_2}=0.279$ ,  $\gamma_{\text{Xe}}=2\gamma_{\text{Xe}_2}=0.007$ . The secondary electron coefficients for the dimer ions were assumed to be  $\gamma_{\text{HeXe}}=\gamma_{\text{Xe}_2}=0.5\gamma_{\text{Xe}}$  and  $\gamma_{\text{He}_2}=0.5\gamma_{\text{He}}$ .

The dependence of the calculated  $V$ - $I$  characteristics on Xe concentration  $N_{\text{Xe}}$ , without inclusion of heteronuclear ion recombination discussed below, is very different from the corresponding dependence of the measured curves.<sup>4</sup> Postel and Cappelli have proposed the formation of  $\text{HeXe}^+$  heteronuclear ions combined with a fast recombination as a mechanism to explain their experimental results.  $\text{HeXe}^+$  ions can indeed be formed by Penning ionization,<sup>19</sup> but mainly through reactions of the type  $\text{He}^++\text{Xe}+\text{He}\rightarrow\text{HeXe}^++\text{He}$  and  $\text{Xe}^++2\text{He}\rightarrow\text{HeXe}^++\text{He}$ , the latter being more favorable. Recombination is represented by the reaction  $\text{HeXe}^++e\rightarrow\text{Xe}^*+\text{He}$ . It should be noted that there are no measurements for the rate coefficients of these reactions and previously reported values are merely best guesses.<sup>14,15</sup> We used our model to study the role of the rate coefficients of the  $\text{HeXe}^+$  formation reaction through three-body collisions of  $\text{Xe}^+$  with He atoms ( $c_1$ ), and of the recombination reaction of  $\text{HeXe}^+$  ( $c_2$ ). In Fig. 2, we show the calculated  $V$ - $I$  characteristics for  $c_1=10^{-29}$  cm<sup>6</sup>/s,  $c_2=8\times 10^{-3}T_e^{-0.5}$  cm<sup>3</sup>/s. Comparison with Fig. 3 of Postel and Cappelli<sup>4</sup> indicates that the dependence of the  $V$ - $I$  curves on  $N_{\text{Xe}}$  is in good agreement with the measurements. The difference in the slope of the  $V$ - $I$  curves for  $N_{\text{Xe}}\geq 0.2N$ , where  $N$  is the gas density, is due to the fact that our model is one-dimensional. One-dimensional models of glow discharges cannot reproduce the constant voltage part of the  $V$ - $I$  characteristic corresponding to a normal glow discharge because they cannot take into account the area through which the current flows.<sup>20</sup>

In addition, we used our excited species kinetics model to compare with the measured VUV emission of Xe excited atoms at 147 nm and of Xe excited dimers at 150 nm by Postel and Cappelli. In Figs. 3 and 4, we show the calculated emission efficiency of the discharge for the  $\text{Xe}^*(^3P_1)$  reso-

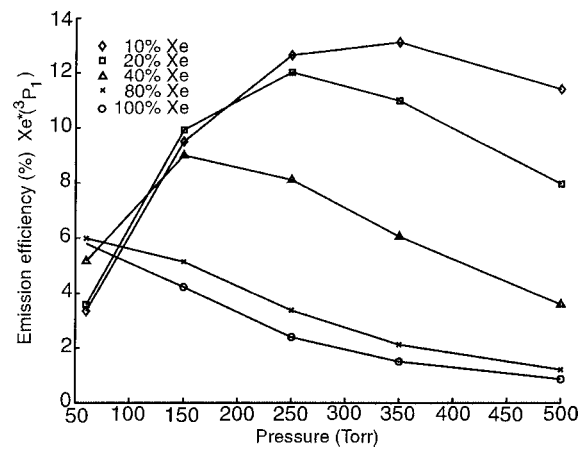


FIG. 3. Calculated emission efficiency from the  $\text{Xe}^*(^3P_1)$  resonant state (147 nm).

nant state (147 nm), and the  $\text{Xe}_2^*(O_u^+)$  excimer (150 nm), respectively, as a function of Xe concentration and total pressure. Comparison with Figs. 4 and 5, respectively, of Postel and Cappelli<sup>4</sup> indicates that these results are also in good agreement with the measured results with the exception of the resonant emission for  $N_{\text{Xe}}=0.1N$ , which is found to be significantly higher in comparison with the experimental result. In addition, features like the local maxima of the resonant emission and their shifting to lower pressures as Xe concentration increases are well reproduced.

The measured  $V$ - $I$  characteristics and Paschen curves reported by Postel and Cappelli suggest that the breakdown voltage for He-Xe mixtures with Xe concentration as low as 10% is closer to the pure Xe breakdown voltage than the pure He breakdown voltage. This dependence is not reproduced by our model unless unusually high (i.e.,  $10^2$  and  $10^5$  times higher, respectively, than the measured values for the corresponding reactions of  $\text{NeXe}^+$  ions in Ne-Xe mixtures<sup>5</sup>) reaction coefficients are used for the formation reaction and the recombination reaction of  $\text{HeXe}^+$  ions. These values are also  $10^3$  and  $5\times 10^4$  times higher, respectively, than the corresponding values guessed by Alford *et al.*<sup>14</sup> on the basis of dependence of specific parameters of He-Xe mixture gas lasers on the constituent gases' concentrations. Use of lower values for  $c_1$  or  $c_2$  results in complete disagreement between

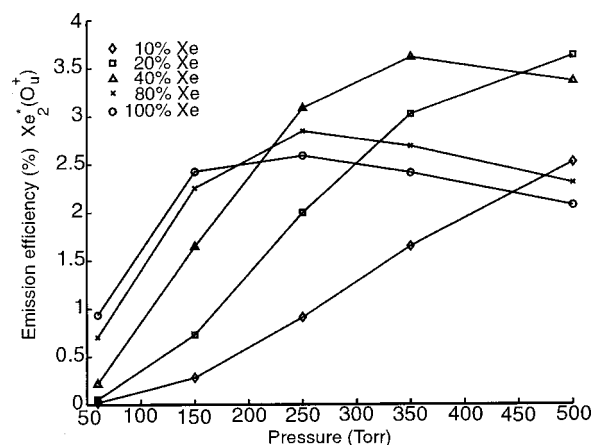


FIG. 4. Calculated emission efficiency from the  $\text{Xe}_2^*(O_u^+)$  excimer state (150 nm).

experimental and simulation results. For example, for  $N_{Xe} = 0.1N$  reduction of either  $c_1$  or  $c_2$  by an order of magnitude shifts the  $V-I$  characteristic by  $\sim 55$  V. We further note that the dependence of breakdown voltage on Xe concentration measured by Postel and Cappelli does not agree with the calculated theoretical results of Uchida *et al.*<sup>17</sup> for Xe concentrations  $< 10\%$ . In this connection, it is important to note that the ionization efficiency calculated by the model of Uchida *et al.* for He–Xe mixtures is in good agreement both with the measured effective ionization efficiency reported by Takahashi and Tachibana<sup>18</sup> and with results obtained using ELENDF, as we already mentioned above.

The model study reported in this letter was motivated by recent experimental work of Postel and Cappelli.<sup>4</sup> The inclusion of heteronuclear ion formation and recombination processes, as originally suggested by Postel and Cappelli,<sup>4</sup> allowed us to achieve a remarkable agreement between our model results and the experiment for the entire range of parameters studied. We note, however, that the required rate coefficients appear to be several orders of magnitude higher than similar rates measured experimentally.<sup>5</sup> These high reaction rates are also in apparent disagreement with previous experimental and theoretical results.<sup>17,18</sup>

This research was supported by the Office of Technology Licensing of Stanford University under Grant No. 127P316. The authors greatly appreciate discussions with Dr. Postel and Dr. Cappelli of the Stanford Mechanical Engineering Department.

<sup>1</sup>A. Sobel, *Sci. Am.* **278**, 70 (1998).

<sup>2</sup>*Electronic Display Devices*, edited by S. Matsumoto (Wiley, New York, 1990), p. 131.

<sup>3</sup>*Excimer Lasers*, edited by C. K. Rhodes (Springer, Berlin, 1979), p. 106.

<sup>4</sup>O. B. Postel and M. A. Cappelli, *Appl. Phys. Lett.* **76**, 544 (2000).

<sup>5</sup>J. Meunier, Ph. Belenguer, and J. P. Boeuf, *J. Appl. Phys.* **78**, 731 (1995).

<sup>6</sup>C. Punset, J. P. Boeuf, and L. C. Pitchford, *J. Appl. Phys.* **83**, 1884 (1998).

<sup>7</sup>J. P. Boeuf, *J. Appl. Phys.* **63**, 1342 (1988).

<sup>8</sup>W. L. Morgan and B. M. Penetrante, *Comput. Phys. Commun.* **58**, 127 (1990).

<sup>9</sup><http://www.sni.net/siglo/database/xsect/siglo.sec>

<sup>10</sup>H. W. Ellis, R. Y. Pai, E. W. McDaniel, E. A. Mason, and L. A. Viehland, *At. Data Nucl. Data Tables* **17**, 177 (1976); H. W. Ellis, E. W. McDaniel, D. L. Albritton, L. A. Viehland, S. L. Lin, and E. A. Mason, *ibid.* **22**, 179 (1978); H. W. Ellis, M. G. Thackston, E. W. McDaniel, and E. A. Mason, *ibid.* **31**, 113 (1984).

<sup>11</sup>S. Rauf and M. J. Kushner, *J. Appl. Phys.* **85**, 3460 (1999).

<sup>12</sup>K. Takahashi, S. Hashiguchi, Y. Murakami, M. Takei, K. Itoh, K. Tachibana, and T. Sakai, *Jpn. J. Appl. Phys., Part 1* **35**, 251 (1996).

<sup>13</sup>H. S. Jeong, B. J. Shin, and K. W. Whang, *IEEE Trans. Plasma Sci.* **27**, 171 (1999).

<sup>14</sup>W. J. Alford, G. N. Hays, M. Ohwa, and M. J. Kushner, *J. Appl. Phys.* **69**, 1843 (1991).

<sup>15</sup>N. G. Basov, V. A. Danilychev, A. Y. Dudin, D. A. Zayarnyi, N. N. Ustinovskii, I. V. Kholin, A. Y. Chugunov, and P. N. Lebedev, *Sov. J. Quantum Electron.* **14**, 1158 (1984).

<sup>16</sup>T. Straaten and M. J. Kushner, *J. Appl. Phys.* **87**, 2700 (2000).

<sup>17</sup>S. Uchida, H. Sugawara, Y. Sakai, T. Watanabe, and B. H. Hong, *J. Phys. D* **33**, 62 (2000).

<sup>18</sup>K. Takahashi and K. Tachibana, *Trans. Inst. Electr. Eng. Jpn., Part A* **111**, 182 (1991).

<sup>19</sup>Y. Tanaka, K. Yoshino, and D. E. Freeman, *J. Chem. Phys.* **62**, 4484 (1975).

<sup>20</sup>Y. P. Raizer, *Gas Discharge Physics* (Springer, Berlin, 1997), p. 181.